THE CHOICE OF CELL FACE VELOCITIES IN THE THREE DIMENSIONAL INCOMPRESSIBLE FLOW CALCULATIONS ON NONORTHOGONAL GRIDS

Seok Ki Choi*, Ho Yun Nam* and Mann Cho*

(Received March 7, 1992)

The effect of choice of cell face velocities on the solution behaviours in the three dimensional incompressible flow calculations on nonorthogonal grids are investigated in detail. The calculation schemes based on the curvilinear contravariant and covariant cell face velocities are developed and are applied to the test problems to assess their relative performances. It is observed that the accuracy of the converged solution is not affected by the different choice of cell face velocities. However, the scheme based on the covariant cell face velocities shows better convergence behaviours when the numerical grids are strongly nonorthogonal.

Key Words: Finite Volume Method, Momentum Interpolation Method, SIMPLE Numerical Algorithm, Cell Face Velocities, Contravariant Velocities, Covariant Velocities

1. INTRODUCTION

In recent years several calculation methods (Shyy, Tong and Correa, 1985, Maliska and Raithby, 1984, Rhie and Chow, 1983, Karki and Patankar, 1988) which employ the nonorthogonal body-fitted coordinates have been developed for a better resolution of fluid flow and heat transfer in domains of irregular boundaries. The development of an efficient calculation method which provides better convergence and accuracy is particularly important for the practical three dimensional calculations. In the SIMPLE family (Patankar, 1980) of calculation methods which are now predominantly used in the incompressible calculations, the solution behaviours are greatly influenced by the treatment of pressure or pressure correction equations. When the numerical grids are nonorthogonal, the derivation of pressure or pressure correction equations is closely related to the choice of cell face velocities. Thus, a proper treatment of pressure and velocity coupling through an adequate choice of cell face velocities is very important for the development of a better calculation method on nonorthogonal grids.

The cell face velocities in the nonorthogonal coordinate system can be either the Cartesian velocity components or the curvilinear contravariant or covariant velocity components. The use of Cartesian velocity components as cell face velocities requires more computer storages and more complicated programings since all the Cartesian velocity components should be stored at each of the cell face locations in order to properly compute the mass fluxes. These disadvantages are particularly grave in the practical three dimensional calculations. The mass fluxes at the cell face locations may be adequately evaluated by employing the contravariant velocity components as cell face velocities.

However, the momentum equations for the contravariant velocity components contain the nonorthogonal pressure gradient terms and the resulting pressure or pressure correction equations are very complicated and may lack in diagonal dominance when the numerical grids are strongly nonorthogonal. In most of the previous calculation methods, the nonorthogonal pressure correction terms are neglected to provide a simple and diagonal dominant pressure correction equation. However, this practice may cause the undesired stability problems when the numerical grids are strongly nonorthogonal and can not be efficiently implemented in the SIMPLER algorithm of Patankar(1980) in which the solution of exact pressure equation is required. These difficulties can be avoided if one uses the curvilinear covariant velocity components as cell face velocities since the momentum equations for the curvilinear covariant velocity components do not contain the cross derivative pressure terms. The scheme employing the curvilinear covariant cell face velocities always provides simple and diagonal dominant pressure and pressure correction equations. However, this practice is not free of difficulties since parts of mass fluxes at the cell face locations should be evaluated through the interpolation of neighbouring velocities. The resulting pressure correction equation involves an additional mass source term which becomes larger with the increase of grid nonorthogonality and hampers the convergence to the machine accuracy.

The objective of the present study is to investigate how the different choice of cell face velocities affects the convergence behaviours and the accuracy of solution in the three dimensional incompressible flow calculations on nonorthogonal grids. As a contemporary study, the present authors(1992) have performed similar investigations for the two dimensional case. Such an effort is further extended to the three dimensional situation in the present study.

The modified Rhie and Chow's scheme(1983) is employed for the present purpose. The original scheme has been modified to remove the relaxation factor dependency of the converged solutions and to take into account the cross derivative pressure terms in evaluating the cell face contravariant velocity components. In this scheme, the momentum equa-

*Fast Breeder Reactor Coolant Department, Korea Atomic Energy Researth Institute, P.O.Box 7, Daeduk-Danji, Taejon, 305-606, Korea

tions are solved at the cell-centered locations using the Cartesian velocity components as dependent variables and the curvilinear cell face velocities are obtained explicitly through the interpolation and algebraic manipulation of the momentum equations for the neighbouring cell-centered Cartesian velocity components rather than solving them implicitly at the cell face locations. This practice removes all the undesiered problems associated with employing the curvilinear velocity components as dependent variables for the momentum equations.

Two computer codes each based on the contravariant and the covariant cell face velocities are developed and are applied to the test problems to assess their relative performances. The convergence behaviours and the accuracy of the converged solution are examined varying the degree of nonorthogonality of numerical grids.

2. FINITE VOLUME FORMULATION

2.1 Governing Equations

The continuity equation and the conservation form of transport equation for a general dependent variable ϕ in the generalized coordinate system x^j can be written as follows

$$\frac{\partial}{\partial x^j}(\rho U_j)=0 \tag{1}$$

$$\frac{\partial}{\partial x^j}(\rho U_j\phi-\frac{\Gamma_\phi}{J}D_m{}^j\frac{\partial\phi}{\partial x^m})=JS_\phi \tag{2}$$

where the contravariant velocity components U_j and the geometric coefficients $D_m{}^j$ are defined as

$$U_j=b_k{}^j u_k \tag{3}$$

$$D_m{}^j=b_k{}^j b_k{}^m \tag{4}$$

and the geometric coefficients $b_i{}^j$ represent the cofactors of $\partial y^i/\partial x^j$ in the Jacobian matrix of the coordinate transformation $y^i=y^i(x^j)$ and J is the determinant of the Jacobian matrix. In these equations, ρ is the density of fluid, Γ_ϕ is the diffusion coefficient of varible ϕ, u_i are the Cartesian velocity components in y^i directions and S_ϕ denotes the source term of variable ϕ.

2.2 Discretization of Transport Equations

The computational domain is subdivided into a finite number of hexahedral control volumes as shown in Fig. 1 and all the variables are stored at the geometric center of each control volume cell. The discretization of transport equations is performed in the physical solution domain following the finite volume approach. The governing equations are integrated over the control volume and the convection terms and the normal diffusion terms are approximated by the power-law profiles of Patankar(1980) and the cross derivative diffusion terms are evaluated explicitly as an additional source term. The resulting algebraic equations for a variable ϕ can be written in the following general form.

$$A_P\phi_P=A_E\phi_E+A_W\phi_W+A_N\phi_N+A_S\phi_S+A_T\phi_T+A_B\phi_B+b_\phi \tag{5}$$

where

$$A_P=A_E+A_W+A_N+A_S+A_T+A_B-S_\phi^P\Delta V \tag{6}$$

$$b_\phi=S_\phi^c\Delta V+S_\phi^b \tag{7}$$

and S_ϕ^b is the source term of a variable ϕ arising due to the nonorthogonality of numerical grid and S_ϕ^c, S_ϕ^P are the linearized source terms.

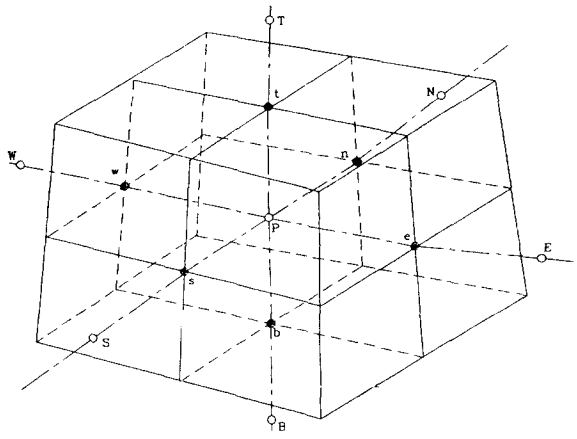

Fig. 1 A typical control volume

3. MOMENTUM INTERPOLATION METHOD

In the present modified Rhie and Chow's scheme, the momentum equations are solved implicitly at the cell-centered locations using the Cartesian velocity components as dependent variables. The discretized form of momentum equations for the cell-centered Cartesian velocity components u_i can be written as follows with the under-relaxation factor expressed explicitly

$$(u_i)_P=(H_{u_i})_P+(Du_i^1)_P(P_w-P_e)+(D_i^2)_P(P_s-P_n)+(Du_i^3)_P(P_b-P_t)+(1-\alpha)(u_i^{n-1})_P \tag{8}$$

where

$$H_{u_j}=\alpha(\sum_{nb}A_{nb}^{u_i}\ u_i^{nb}+b_{u_j})/A_P^{u_i} \tag{9}$$

$$D_{u_i}^j=\alpha b_i^j/A_P^{u_i} \tag{10}$$

and α is the under-relaxation factor and the superscript $(n-1)$ denotes the previous iteration level.

In order to compute the mass fluxes through the cell faces, it is necessary to compute the velocities at the cell face location. The discretized form of momentum equations for the cell face Cartesian velocity components, for example at the east face, can be written as follows

$$(u_i)_e=(H_{u_i})_e+(D_{u_i}^1)_e(P_P-P_E)+(D_{u_i}^2)(P_{se}-P_{ne})+(D_{u_i}^3)_e(P_{be}-P_{te})+(1-\alpha)(u_i^{n-1})_e \tag{11}$$

In the conventional staggered grid method, above momentum equations for the cell face velocity components are implicitly solved with algebraic coefficients evaluated at the cell face locations. In the present modified Rhie and Chow's scheme, these cell face Cartesian velocity components are obtained through the interpolation of momentum equations for the neighbouring cell centered Cartesian velocity components, Eq. (8). Following assumptions are introduced to evaluate these cell face velocites, for example u_i at the east cell face.

$$1/(A_P^{u_i})_e\approx f_e^+/(A_P^{u_i})_E+(1-f_e^+)/(A_P^{u_i}) \tag{12}$$

$$(H_{u_i})_e\approx f_e^+(H_{u_i})_E+(1-f_e^+)(H_{u_i})_P \tag{13}$$

where f_e^+ is the geometric interpolation factor defined in terms of distances between nodal points.

$$f_e^+=\overline{Pe}/(\overline{Pe}+\overline{eE}) \tag{14}$$

Similar assumptions can be introduced for the evaluation of the velocity components at the other cell face locations. The accuracy of these assumptions may be affected by the flow situation and the grid nonorthogonality unless the numerical grids are fine enough.

4. PRESSURE CORRECTION SCHEME

In the present study, the coupling between the continuity and the momentum equations is effected using the SIMPLE algorithm of Patankar(1980). Followings are the details of pressure correction sheme in the modified Rhie and Chow's scheme associated with employing different cell face velocities.

4.1 Contravariant Cell Face Velocities Based Scheme

The integrated continuity equation for a control volume cell around a grid point P, shown in Fig. 1, can be written as

$$(\rho U_1)_e-(\rho U_1)_w+(\rho U_2)_n-(\rho U_2)_s+(\rho U_3)_t-(\rho U_3)_b=0 \tag{15}$$

The momentum equations for the contravariant cell face velocity components can be derived by substituting the momentum equations for the cell face Cartesian velocity components, Eq. (11), to the relations between two velocity components, Eq. (3). The resulting equations are as follows.

$$(U_1)_e=(\hat{U}_1)_e+(D_{U_1^1})_e(P_P-P_E)+(D_{U_1^2})_e (P_{se}-P_{ne})+(D_{U_1^3})_e(P_{be}-P_{te}) \tag{16}$$

$$(U_2)_n=(\hat{U}_2)_n+(D_{U_2^1})_n(P_{wn}-P_{en})+(D_{U_2^2})_n (P_P-P_N)+(D_{U_2^3})_n(P_{bn}-P_{tn}) \tag{17}$$

$$(U_3)_t=(\hat{U}_3)_t+(D_{U_3^1})_t(P_{wt}-P_{et})+(D_{U_3^2})_t (P_{st}-P_{nt})+(D_{U_3^3})_t(P_P-P_T) \tag{18}$$

where

$$\hat{U}_i=b_k^i H_{u_k}+(1-\alpha)\,U_i^{n-1} \tag{19}$$

$$D_{U_i}^j=b_k^i D_{u_k}^j \tag{20}$$

It is noted that these cell face contravariant velocity components are evaluated explicitly using the assumptions given in Eqs. (12) ~ (13) with the geometric coefficients evaluated at the cell face locations.

The velocity components obtained by Eqs. (16) ~ (18) will, in general, not satisfy the mass conservation unless the pressure field is correct. These starred velocity components are corrected to satisfy the continuity equation by following velocity correction equations.

$$(\Delta U_1)_e=(U_1-U_1^*)_e=(D_{U_1^1})_e(P_P'-P_E') \tag{21}$$

$$(\Delta U_2)_n=(U_2-U_2^*)_n=(D_{U_2^2})_n(P_P'-P_N') \tag{22}$$

$$(\Delta U_3)_t=(U_3-U_3^*)_t=(D_{U_3^3})_t(P_P'-P_T') \tag{23}$$

where p′ is the pressure correction.

The nonorthogonal pressure correction terms are neglected to obtain a simple and diagonal dominant pressure correction equation. Substitution of these velocity correction formula into the continuity equation, Eq. (15), results in an equation for pressure correction.

$$A_P^N P_p=\sum_{nb} A_{nb}^N P_{nb}+b_N \tag{24}$$

where

$$b_N=(\rho U_1^*)_w-(\rho U_1^*)_e+(\rho U_2^*)_s-(\rho U_2^*)_n+(\rho U_3^*)_b-(\rho U_3^*)_t \tag{25}$$

One can notice that the present contravariant cell face velocities based scheme is slightly different from that reported in Peric(1985).

4.2 Covariant Cell Face Velocities Based Scheme

The physical covariant velocity components V_i are related to the Cartesian velocity components u_j as

$$V_i=\bar{e}_{x^i}\cdot\bar{u}=u_j\frac{\partial y^j}{\partial x^i}/(g^{ii})^{1/2} \text{ (ii not summation)} \tag{26}$$

where $\bar{e}_{x^i}$ are the unit vectors in x^i directions and the geometric coefficients g^{ii} are defined as

$$g^{ii}=\frac{\partial y^j}{\partial x^i}\frac{\partial y^j}{\partial x^i} \quad \text{(ii not summation)} \tag{27}$$

The contravariant velocity components U_i can be expressed in terms of the covariant velocity components V_j as

$$U_i=\alpha_{ij}V_j \tag{28}$$

where α_{ij} are the geometric coefficients defined as

$$\alpha_{ij}=\frac{1}{J}D_j^i/(g^{jj})^{1/2} \quad \text{(jj not summation)} \tag{29}$$

With these relations, the continuity equation can be rewritten as

$$(\rho\alpha_{11}V_1)_e-(\rho\alpha_{11}V_1)_w+(\rho\alpha_{22}V_2)_n-(\rho\alpha_{22}V_2)_s+(\rho\alpha_{33}V_3)_t-(\rho\alpha_{33}V_3)_b=b_{NO} \tag{30}$$

where b_{NO} is the nonorthogonal mass source term arising due to the choice of the covariant velocity components as cell face velocities and is defined as

$$b_{NO}=(\rho\alpha_{12}V_2+\rho\alpha_{13}V_3)_w-(\rho\alpha_{12}V_2+\rho\alpha_{13}V_3)_e+(\rho\alpha_{21}V_1+\rho\alpha_{23}V_3)_s-(\rho\alpha_{21}V_1+\rho\alpha_{23}V_3)_n+(\rho\alpha_{31}V_1+\rho\alpha_{32}V_2)_b-(\rho\alpha_{31}V_1+\rho\alpha_{32}V_2)_t \tag{31}$$

The momentum equations for the covariant cell face velocity components can be derived through the algebraic manipulation of equations like Eq. (11) and Eq. (26).

$$(V_1)_e=(\hat{V}_1)_e+(D_{V1})_e(P_P-P_E) \tag{32}$$

$$(V_2)_n=(\hat{V}_2)_n+(D_{V2})_n(P_P-P_N) \tag{33}$$

$$(V_3)_t=(\hat{V}_3)_t+(D_{V3})_t(P_P-P_T) \tag{34}$$

where

$$\hat{V}_i=H_{u_j}\frac{\partial y^j}{\partial x_i}/(g^{ii})^{1/2}+(1-\alpha)\,V_i^{n-1} \text{ (ii not summation)} \tag{35}$$

$$D_{V_i}=D_{u_j^i}\frac{\partial y^j}{\partial x^i}/(g^{ii})^{1/2} \quad \text{(ii not summation)} \tag{36}$$

The correction equations for the covariant velocity components can be written as

$$(\Delta V_1)_e=(V_1-V_1^*)_e=(D_{V1})_e(P_P'-P_E') \tag{37}$$

$$(\Delta V_2)_n=(V_2-V_2^*)_n=(D_{V2})_n(P_P'-P_N') \tag{38}$$

$$(\Delta V_3)_t=(V_3-V_3^*)_t=(D_{V_3})_t(P_P'-P_T') \tag{39}$$

The pressure correction equation can be derived by substituting these velocity correction equations to the continuity equation, Eq. (30).

$$A_P^c P_P'=\sum_{nb} A_{nb}^c P_{nb}'+b_c+b_{NO} \tag{40}$$

where

$$b_C=(\rho\alpha_{11}V_1^*)_w-(\rho\alpha_{11}V_1^*)_e+(\rho\alpha_{22}V_2^*)_s-(\rho\alpha_{22}V_2^*)_n+(\rho\alpha_{33}V_3^*)_b-(\rho\alpha_{33}V_3^*)_t \tag{41}$$

After solving the pressure correction equation, the pressure and the cell-centered Cartesian velocity components are updated by following equations using the assumption of linearly varying pressure field.

$$P=P^*+\alpha_P P' \tag{42}$$

$$(u_i)_P=(u_i^*)_P+(D_{u_1^1})_P(P_w'-P_e')+(D_{u_1^2})_P(P_s'-P_n')+(D_{u_1^3})_P(P_b'-P_t') \tag{43}$$

The optimal relaxation factor by Peric(1985), $\alpha_P=1-\alpha_u$, is employed for most of the present calculations.

5. APPLICATIONS TO TEST PROBLEMS

Two computer codes based on the contravariant [EL-

CON3D] and the covariant [ELCOV3D] cell face velocities are developed and are applied to the test problems to investigate their relative performances. The test problems include ; fully developed laminar flow in a straight square duct and laminar flow in a lid-driven inclined cubic cavity. The convergence behaviours and the accuracy of the converged solution are examined varying the degree of the grid nonorthogonality. Before conducting these numerical experiments, both codes have been validated through the applications to several test problems such as laminar flows in the ducts of 90 degree and 180 degree bend with circular and square cross sections, and laminar flow in a cubic cavity. Since the results of these problems are not relevant to the objective of the present study, they are not reported here.

5.1 Fully Developed Laminar Flow in a Square Duct

A fully developed laminar flow in a square duct, schematically shown in Fig. 2, is solved varying the degree of nonorthogonality of numerical grid to investigate how the different choice of cell face velocities influences the convergence and accuracy of the solution. These numerical experiments also provide information on the influence of the treatment of cross-derivative diffusion and pressure terms on the accuracy and stability of the scheme. The uniform 21*21*21 grids are generated within a quarter of the duct in which the longitudinal solution domain is extended to five times the half width of duct. Exact fully developed profiles in White(1974) are prescribed at the inlet and zero axial gradient conditions are imposed at the exit. Four cases with different inclinations (β =90, 60, 45, 30) are studied. The Reynolds number based on the half width of duct and the bulk velocity is 100 and the relaxation factors used in the present calculations are $\alpha_u=\alpha_v=\alpha_w=0.7$ and $\alpha_p=0.3$.

Table 1 shows the predicted maximum percentage errors for each case where the maximum error E_{max} is defined as $E_{max}=|u_{cal}-u_{exact}|_{max}/u_{max}$ and u_{max} is the maximum inlet velocity. We can notice that the accuracy of the converged solution is not affected by the different choice of cell face velocities. The maximum percentage error becomes larger with the increase of grid nonorthogonality. However, both codes result in accurate enough solutions even in strongly nonorthogonal grid situations. It is also found that most of the maximum errors are occurred at the last few stations near the exit and except for these regions, the maximum errors are found to be less than 1%. These observations indicate that the predicted numerical errors are somewhat related to the treatment of boundary conditions at the exit rather than to the numerical scheme itself.

Fig. 3 show the convergence histories for four cases with different inclinations. It is noted that there exist strong wiggles in the convergence histories. When these convergence behaviours are compared with those for the inclined cubic cavity flows shown in the next section, these wiggles are somewhat related to the treatment of outflow boundary conditions. The same outflow boundary conditions commonly employed in the well known codes like TEACH or EL2D, EL3D are used in the present calculations. We have also found that these wiggles are related to the relaxation factors used. Our numerical experiments show that the magnitude and the frequency of the wiggles are changed when only the relaxation factor for the pressure correction(α_p) is slightly changed. Fig. 3(d) shows that wiggle free solutions can be obtained depending on the flow situation and relaxation factors used (ELCOV3D, $\beta=30$, $\alpha_u=\alpha_v=\alpha_w=0.7$ and $\alpha_p=0.2$). However, as far as the convergence is reached, the wiggle in the convergence histories is not an important parameter for the overall solution procedure.

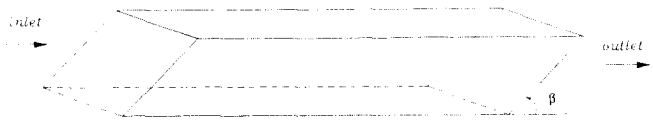

Fig. 2 Fully developed laminar flow in a square duct

Table 1 Maximum percentage errors of u-velocity component

	$\beta=90$	$\beta=60$	$\beta=45$	$\beta=30$
ELCON3D	0.176%	0.723%	1.088%	1.988%
ELCOV3D	0.176%	0.722%	1.087%	1.988%

These figures show that the convergence rate is significantly affected by the different choice of the cell face velocities as well as the degree of grid nonorthogonality. When the numerical grids are orthogonal ($\beta=90$), both codes result in the same convergence histories as expected. However, as the grid nonorthogonality becomes significant, the differences in convergence rates become more pronounced. The ELCOV3D code based on the covariant cell face velocities always shows better convergence behaviours. The ELCON3D code based on the contravariant cell face velocities causes stability problems when the numerical grids are strongly nonorthogonal (β =30). The convergence is achieved only in a limited range of relaxation factors ($\alpha_p<0.2$ when $\alpha_u=\alpha_v=\alpha_w=0.7$). The convergence histories shown in Fig. 3(d) are for the case of $\alpha_u=\alpha_v=\alpha_w=0.7$ and $\alpha_p=0.2$. Peric(1990) has shown that the poor performances of the contravariant cell face velocities based scheme in strongly nonorthogonal grid situations are due to the neglection of the cross derivative pressure correction terms in the contravariant velocity correction equations, Eqs.(21) ~ (23). However, the inclusion of the nonorthogonal pressure correction terms leads to a very complicated pressure correction equation, especially in the three dimensional situation.

5.2 Laminar Flow in a Lid-Driven Cubic Cavity

Laminar flows in a cubic cavity with a moving top wall and inclined side walls, schematically shown in Fig. 4, is solved for Reynols numbers of 100 and 1000 to investigate the accuracy of the schemes and the effect of choice of cell face velocities and grid nonorthogonality on the convergence behaviours.

First, laminar flows in a cubic cavity without inclination (β =90) is solved employing two different numerical grids (32* 32*32, 42*42*42) to examine the accuracy of the schemes. Fig. 5 show the predicted centerline velocity distributions at the center plane together with the calculations by Rosenfeld (1991) and other results given in Rosenfeld(1991). Both codes result in nearly the same converged solutions which are not discernible in the plottings. Thus, only the results by the ELCOV3D code is presented. Good agreements are obtaind for both Reynolds numbers except a slight deviation is observed when the Reynolds number is high (Re= 1000) and the numerical grids are coarse (32*32*32). This may be due to the use of lower order scheme, power-law scheme, in the present study. It is also noted that these errors are reduced with a little grid refinement (42*42*42).

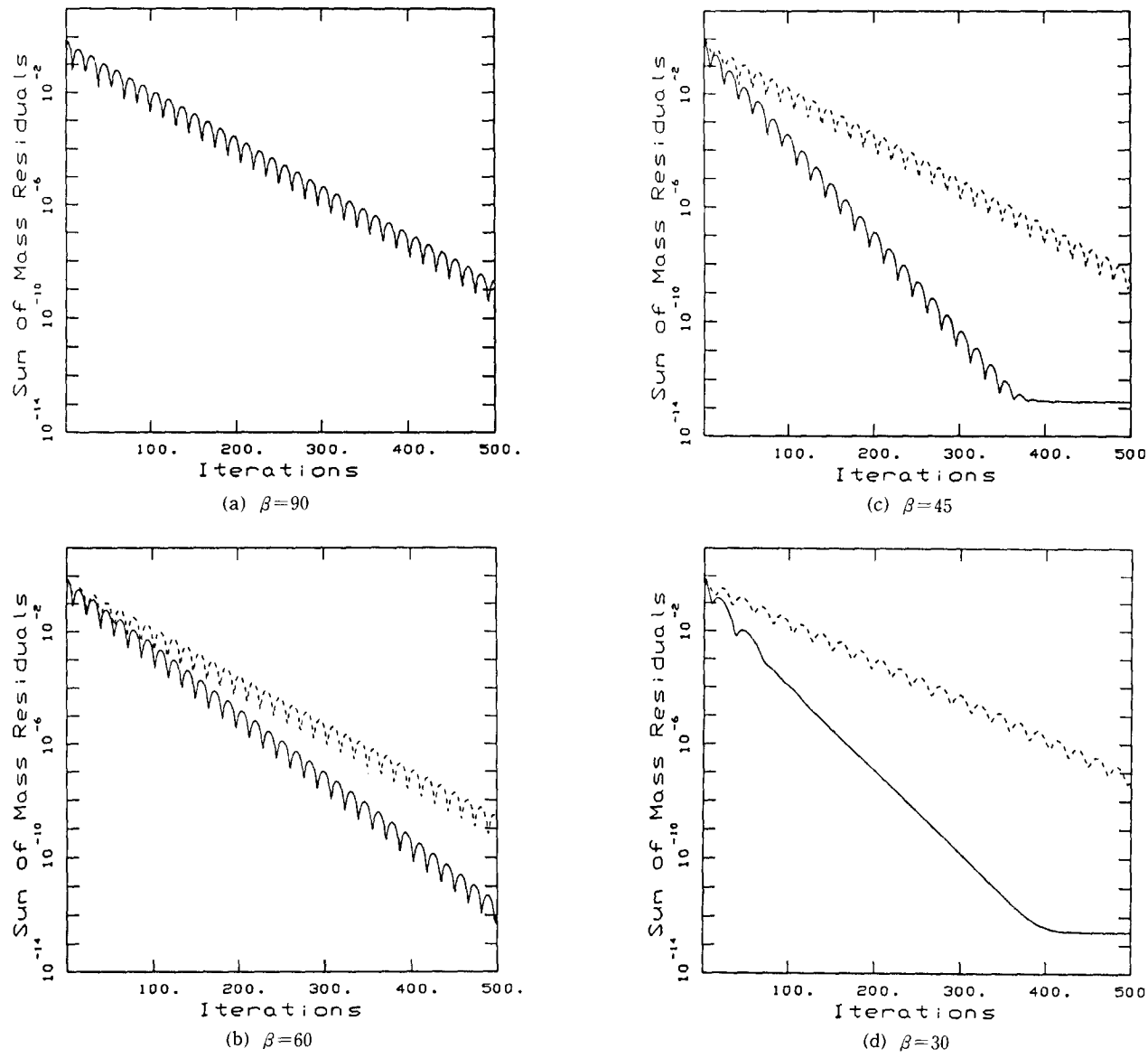

Fig. 3 Convergence histories for duct flows

The effect of choice of cell face velocities on the convergence behaviours are also investigated in this test problem. Like the previous test problem, four cases with different inclinations (β=90, 60, 45, 30) are studied employing 21*21*21 uniform numerical grids. Two different Reynolds numbers, 100 and 1000, based on the wall velocity and the width of top wall are employed to investigate the Reynolds number effect on the solution behaviours.

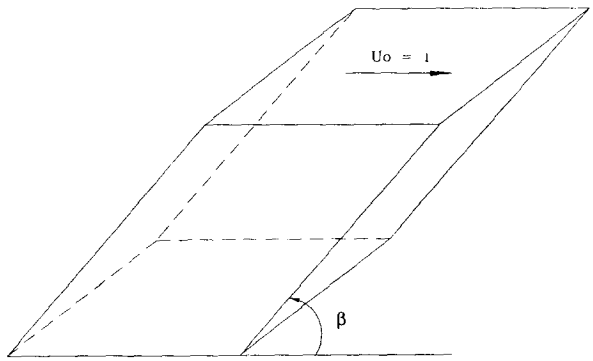

Fig. 4 Laminar flow in a lid-driven cubic cavity

Fig. 6 show the convergence histories of the sum of the normalized mass residuals of pressure correction equation for four cases with different inclinations when the Reynolds number is 100. Unlike the previous test problem, the differences in the convergence rates are not pronounced in this problem although some differences are observed when the numerical grids are strongly nonorthogonal (β=30). These observations show that the relative convergence behaviours associated with employing different cell face velocities are a little problem dependent. We can also observe that these convergence behaviours are a little different from those reported in the present author's earlier work (1992) for the two dimensional inclined cavity problem. The differences in convergence rates will be more pronounced if the geometric

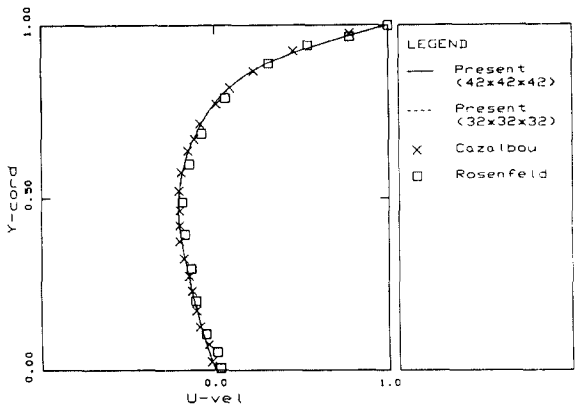

(a) Re=100

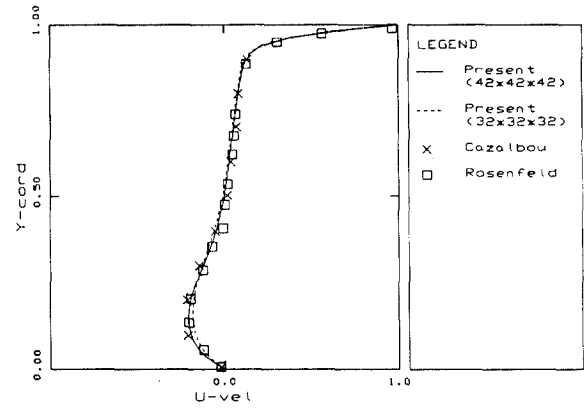

(b) Re=1000

Fig. 5 Centerline velocity distributions

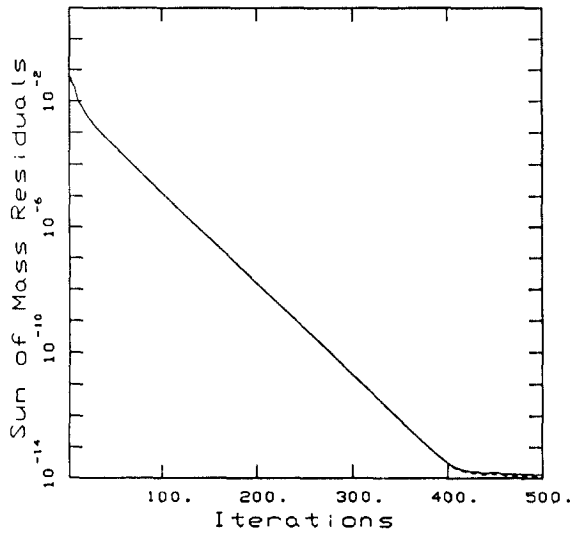

(a) β=90

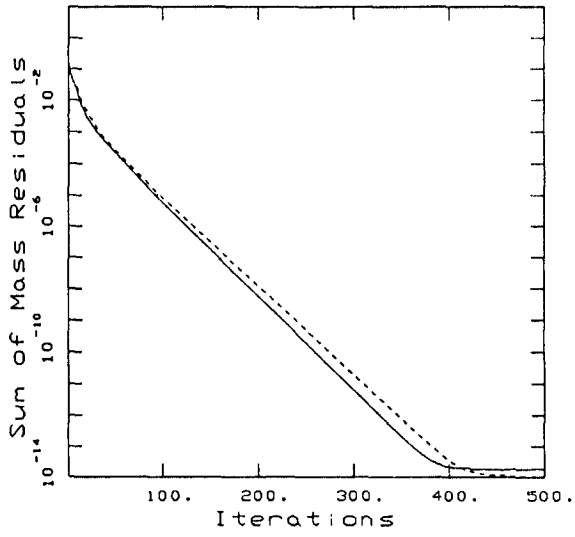

(b) β=60

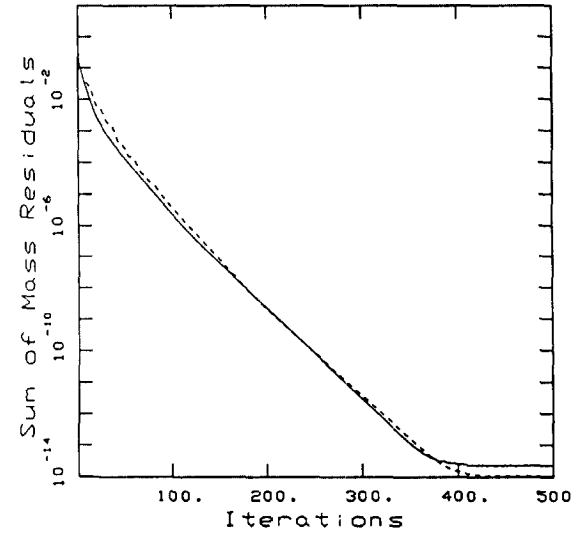

(c) β=45

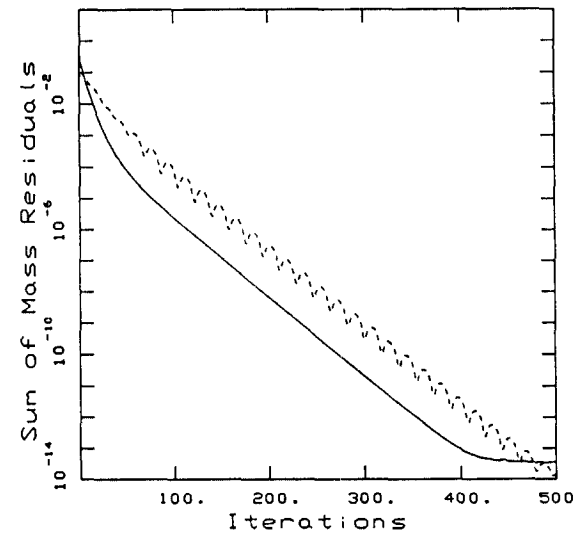

(d) β=30

Fig. 6 Convergence histories for cavity flows : Re=100

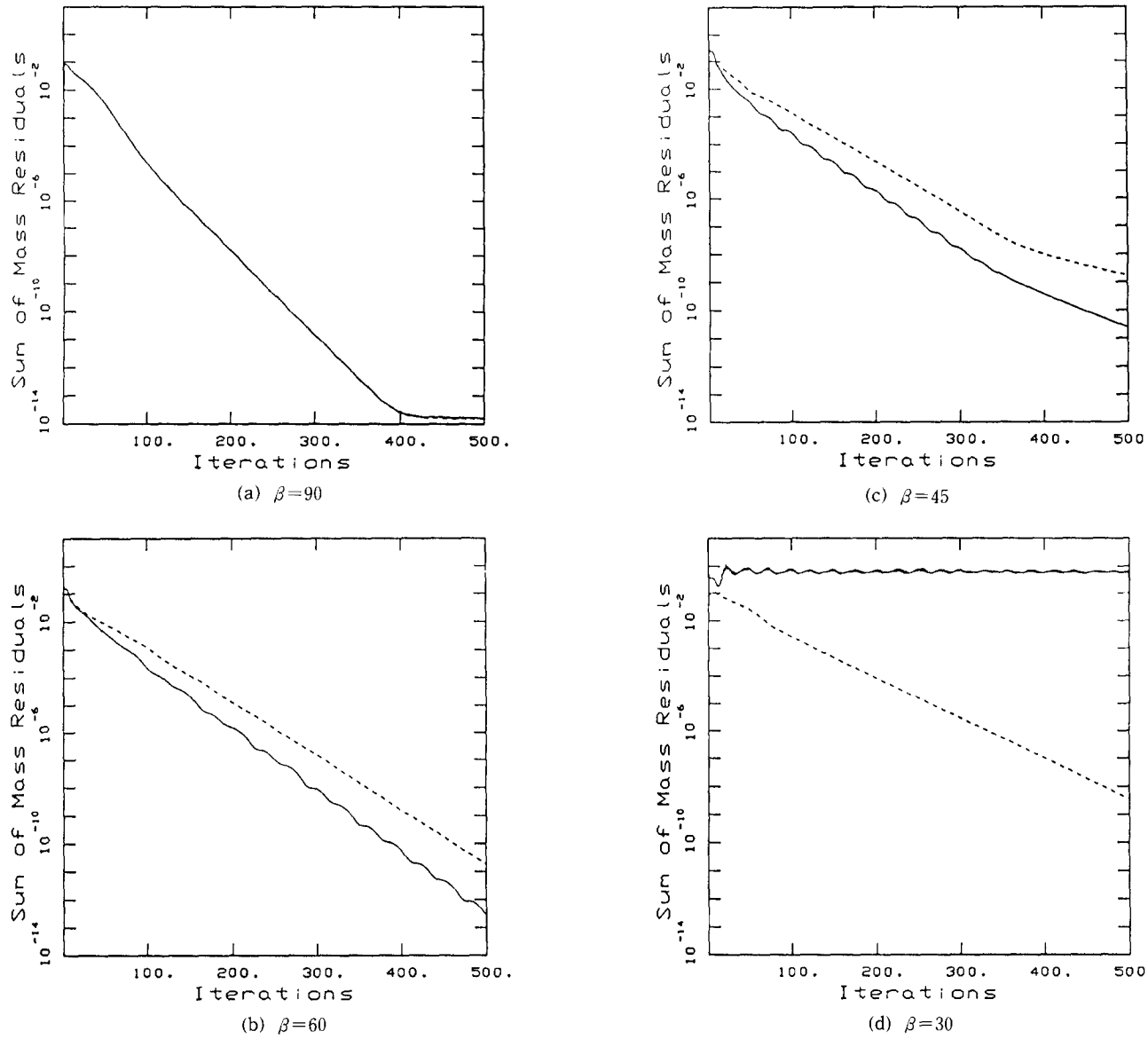

Fig. 7 Convergence histories for cavity flows : Re=1000

shape of the cavity is inclined in two directions. However, the solution by the ELCOV3D code generally shows better convergence behaviours. As shown in Fig. 7, these solution behaviours are not much altered even though the Reynolds number in increased one order higher to Re=1000. The differences in convergence rates are a little more pronounced in this case.

Fig. 6 show that the solution by the ELCOV3D code does not converge to the machine accuracy when the numerical grids are nonorthogonal while the solution by the ELCON3D code always converges to the machine accuracy. This deficiency of the ELCOV3D code is originated from the incomplete convergence of the nonorthogonal mass source term, b_{NO}, in the pressure correction equation, Eq. (40), which is usually obtained through the interpolation of neighbouring velocities. The amount of the incomplete convergence of the nonorthogonal mass source term becomes larger with the increase of grid nonorthogonality. In usual cases, the magnitude of the incomplete convergence is far smaller than the usual accepted convergence criteria even in a strongly nonorthogonal situation and does not influence the accuracy of the final converged solutions as shown in Table 1. However, depending on the flow situation and gird nonorthogonality, there exist possibilities that this additional nonorthogonal mass source term, b_{NO}, becomes so large that the solution fails to converge (but not diverge). A typical example of this case is shown in Fig. 7(d). Our numerical experiments altering the relaxation factors do not change this abnormal convergence behaviours. This fact may be a serious drawback of the covariant cell face velocities based scheme to question that this scheme can be used in the general purpose codes.

6. CONCLUSIONS

Three dimensional calculation procedures for incompressible flows in complex geometries based on the modified Rhie and Chow's scheme with different cell face velocities are

presented. The relative performances between the scheme based on the contravariant cell face velocities and the scheme based on the covariant cell face velocities are examined through the applications to the test problems. Following conclusions emerge from these numerical experiments.

(1) The accuracy of the converged solution is not affected by the different choice of cell face velocities.

(2) As far as convegence is reached, in general, better convergence behaviours are observed when the covariant velocity components are selected as cell face velocities, especially in the strongly nonorthogonal grid situations.

(3) The solutions by the scheme based on the covariant cell face velocities do not converge to the machine accuracy when the numerical grids are nonorthogonal due to the existence of the additional nonorthogonal mass source term. In usual cases, the magnitude of the incomplete convergence is far smaller than the usual accepted convergence criteria even in a strongly nonorthogonal grid situation and does not influence the accuracy of the final converged solutions. However, there exist possiblilities that this additional nonorthogonal mass source term becomes too large to reach the convergence.

REFERENCES

Choi, S. K., Nam, H. Y. and Cho, M., 1992, "On the Use of Momentum Interpolation Method for the Numerical Solution of Incompressible Flows in Complex Geometries : The Choice of Cell Face Velocities," Numer. Heat Transfer, Part B, In Press.

Karki, K.C. and Patankar, S.V., 1988, "Calculation Procedure for Viscous Incompressible Flows in Complex Geometries," Numer. Heat transfer, Vol. 14, pp. 295~307.

Maliska, C.R. and Raithby, G.D., 1984, "A Method for Computing Three-Dimensional Flows Using Non-Orthogonal Boundary-Fitted Coordinates," Int. J. Numer. Methods. Fluids, Vol. 4, pp. 519~537.

Patankar, S.V., 1980, "Numerical Heat Transfer and Fluid Flow," McGraw-Hill, New York.

Peric, M., 1985, "A Finite Volume Method for the Prediction of Three Dimensional Fluid Flow in Complex Ducts," Ph. D Thesis, University of London.

Peric, M., 1990, "Analysis of Pressure-Velocity Coupling on Nonorthogonal Grids," Numer. Heat Transfer, Part B, Vol. 17, pp. 63~82.

Rhie, C.M. and Chow, W.L., 1983, "Numerical Study of the Turbulent Flow Past an Airfoil with Trailing Edge Separation," AIAA J., Vol. 21, No. 11, pp. 1525~1532.

Rosenfeld, M., Kawk, D. and Vinokur, M., 1991, "A Fractional Step Solution Method for the Unsteady Incompressible Navier Stokes Equation in Generalized Coordinate System," J. Comput. Physics, 94, pp. 102~137.

Shyy, W., Tong, S.S. and Correa, S.M., 1985, "Numerical Recirculating Flow Calculations Using a Body-Fitted Coordinate System," Numer. Heat Transfer, Vol. 8, pp. 99~113.

White, F.M., 1974, "Viscous Fluid Flow," McGraw-Hill, New York, pp. 123.